JOURNAL OF MATERIALS SCIENCE 31 (1996) 54–60

Attack of $YBa_2Cu_3O_{6.8}$ by acidic aqueous solutions

R. J. CANDAL, M. A. BLESA
INQUIMAE, Facultad de Ciencias Exactas, Universidad de Buenos Aires, Ciudad Universitaria, Pabellón 2, 1428-Buenos Aires, Argentina

A. E. REGAZZONI
Departamento Química de Reactores, Comisión Nacional de Energía Atómica, Av. del Libertador 8250, 1429-Buenos Aires, Argentina

The dissolution of $YBa_2Cu_3O_{6.8}$ in acidic aqueous solutions was studied at 298 K as a function of pH, nature and concentration of present anions and time, t. In the range $2.0 \leq pH \leq 4.0$, dissolution is congruent and proceeds to completion; dissolution profiles are deceleratory and comply with a contracting volume rate law up to $t_{0.5}$. The rate of dissolution, which is limited by slow surface reactions, decreases with increasing pH; the kinetic order on proton concentration is a fractional and variable number. At higher pH values, dissolution is arrested at intermediate conversion values. In these cases, congruent dissolution is followed by the precipitation of less soluble solid phases which form a passive layer. The nature of this passive layer depends on pH and on the nature and concentration of present anions, which also define the extent of conversion attained at passivation. The dissolution behaviour of $YBa_2Cu_3O_{6.8}$ is described in terms of two consecutive surface reactions: fast equilibrated protonation of surface metal ions is followed by the slow release of cations. Barium surface ions are identified as the more reactive sites. The effect of the fast initial leaching of barium ions on the reactivity of yttrium and copper sites is discussed. The influence of the formal Cu(III) oxidation state is also stressed.

1. Introduction

The corrosion of high critical temperature, T_c, superconducting oxide phases by water has received considerable attention during the last years [1, 2]. Most of the published studies refer to high instability of $YBa_2Cu_3O_{7-x}$ in both moist atmospheres and liquid water [1–10]. The high reactivity of $YBa_2Cu_3O_{7-x}$ towards water was found to be determined by the concentration of oxygen vacancies [4, 11, 12], the average copper oxidation state [6, 13] and the presence of an alkali earth cation in the crystal structure [4, 11, 13]. At present it is well established that water chemisorbes dissociatively and that the resulting OH^- species penetrate the solid lattice via an oxygen vacancy mechanism [4, 11], giving rise to the formation of planar defects normal to the c-axis [3, 4]; further water penetration produces extended damage of the crystal microstructure and eventually leads to the collapse of the lattice [5]. More recently, Rupeng *et al.* [12] have shown that the planar defects are formed by the hydroxylation of Cu(1)–O chains which split into two $Cu_{1/2}(OH)$ chains; the latter stack between Ba–O planes in a way that resembles the sequence found in $YBa_2Cu_4O_8$.

While most of the previous studies focus their attention on the solid state aspects of the corrosion process, it is clear that the solvent is an essential reagent in the corrosion reaction. As such, its composition should be, at least, as important as solid state factors in determining dissolution and/or corrosion rates. Indeed, the site of the attack is the interface, its properties being defined by both phases, the solid and the solution. However, only few works report on the influence of solution composition on corrosion rates, attempting mainly to unravel the electrochemistry of $YBa_2Cu_3O_{7-x}$ electrodes [14–17]. The experimental evidence indicates that protons [14, 18, 19], as well as the nature of the counter-ion [20], play a major role in the corrosion reaction.

With the aim of establishing the actual role played by protons and anions, a kinetic study of the dissolution of $YBa_2Cu_3O_{6.8}$ in acidic aqueous solutions of various compositions is presented.

2. Experimental procedure

$YBa_2Cu_3O_{6.8}$ was prepared following the well established route of solid state synthesis; high purity (AR grade) $BaCO_3$, CuO and Y_2O_3, mixed in the appropriate amounts, were used as starting materials. The X-ray diffraction (XRD) pattern of the resulting powder corresponded to orthorhombic $YBa_2Cu_3O_{7-x}$;

0022–2461

no other solid phases could be detected by XRD. The Brunauer–Emmett–Teller (BET) specific surface area of the powder, determined from the N_2 adsorption isotherm at 77 K, was $2.4 \pm 0.2\ m^2\ g^{-1}$. Scanning electron micrographs showed that the sample was composed of polydispersed irregular particles, their size ranging from ~ 1 to 30 μm.

The chemical composition of the solid was assessed by chemical analyses. Y, Ba and Cu, which were found to comply with the expected 1:2:3 molar ratio, were determined by ionic chromatography. The content of oxygen per formula unit, 6.80 ± 0.01, was determined by bromometric titrations following the procedure described by Crubelatti *et al.* [21].

Dissolution reactions were started by suspending the oxide (75 mg) into solutions (100 cm^3 each) of desired pH and NaCl concentration. Aliquots of these suspensions were withdrawn at different time intervals and filtered through 0.2 μm pore size cellulose acetate membranes. Particle free supernatant solutions were then stored for the chemical assay of dissolved metal ions. In selected cases, the partially reacted solids were rapidly washed with cold water, vacuum dried and stored for scanning electron microscopy (SEM) inspection and energy dispersion spectroscopy (EDX). pH was kept constant throughout the dissolution reactions. For this purpose, 1 mol dm^{-3} HCl was continuously added using a Metrohm 672 titroprocessor in the pH-stat mode.

To investigate the role of the anion of the mineral acid, another set of experiments was performed at pH 5.0. In these cases, dissolution reactions were followed by recording the amounts of the different mineral acids used to keep pH constant.

All dissolution experiments were carried out at 298.0 ± 0.2 K in a thermostated Pyrex reaction vessel. Particles were kept in suspension by means of a magnetic stirrer (700 r.p.m. rotation speed) using a 15 mm Teflon coated stirring bar. When necessary, carbon dioxide was excluded from the reacting systems by bubbling CO_2-free nitrogen. All solutions were made up using AR grade reagents and deionized water obtained from a Milli-Q apparatus (conductivity less than 0.1 μS cm^{-1}).

The concentrations of dissolved Y, Ba and Cu were determined by atomic absorption spectroscopy (AAS) in a Varian AA5 instrument; acetylene and nitrous oxide were used as fuel and comburent, and when necessary KCl was added as an ionization suppressor. Alternatively, when the concentrations of the metal ions were below the AAS detection limit, they were assessed by ionic chromatography following the procedure developed by Gautier *et al.* [22]; a Konik KNK-500A apparatus, equipped with a 0.1 cm^3 sample loop, a linear ultra violet (U.V.) 204 detector and a Vydac 302IC4.6 silica based exchange column, was employed. 1.2×10^{-3} mol dm^{-3} cyclohexylendiaminotetraacetic acid solution was used as eluent [22].

3. Results

The dissolution of $YBa_2Cu_3O_{6.8}$ in aqueous media is highly dependent on the composition of the solution. This is illustrated in Fig. 1a–e, which shows the kinetics of the uptake of Y, Ba and Cu by the studied media; results in Fig. 1 are cast in terms of dissolved fraction ($f = C/C^\infty$, where C and C^∞ denote the concentration of either metal ion at a given time, t, and at complete dissolution, respectively). In the range pH ≤ 4.0, all metal ions dissolve at the same rate, and the reaction proceeds to completion (see Fig. 1a and b). Thus, dissolution is congruent; its stoichiometry is given by

$$YBa_2Cu_3O_{6.8} + 13H^+ \rightarrow Y^{3+} + 2Ba^{2+} + 3Cu^{2+} + 6.5H_2O + 0.15O_2 \quad (1)$$

The above process was found to comply with a contracting volume rate law (Equation 2) up to $f \approx 0.5$. This is shown in Fig. 2, which presents the $[1-(1-f)^{1/3}]$ versus t plot for the experiment carried out at pH 4.0. Deviations from

$$(1-f)^{1/3} = 1 - kt \quad (2)$$

where k is the rate determining constant (which are not shown in Fig. 2) should be, at least partially, a result of the polydispersity of the sample; fines, that dissolve faster, alter the shape of f versus t plots, particularly at high conversion values [23, 24]. At pH values lower than 4.0, compliance with Equation 2 is similar. Table I collects k values derived from the linear portions of $[1-(1-f)^{1/3}]$ versus t plots for pH ≤ 4.0.

Rate constants, k, can be further elaborated [24] to yield the more fundamental specific rate per unit area

$$R_s = \frac{r_0 \rho}{M} k \quad (3)$$

and penetration rate

$$p = r_0 k \quad (4)$$

where r_0 is the initial radius of the particles, M is the molecular weight of the oxide and ρ is its density. Even though the polydispersity of the sample precludes the accurate determination of these magnitudes, they can be estimated using the specific surface area, assuming that particles are monosized spheres. The values so estimated are also included in Table I.

The figures presented in Table I demonstrate that dissolution proceeds at rates that are lower than the solution diffusion control limit. For this limit, the estimated values of k (Equation 5) range between 2.7×10^{-1} and $2.7 \times 10^{-3}\ s^{-1}$.

$$k_{diff}/s^{-1} = \frac{DM}{\delta r_0 \rho}[H^+] = 27[H^+] \quad (5)$$

where $[H^+]$ is the bulk proton concentration, $D = 5.0 \times 10^{-6}\ cm^2\ s^{-1}$ is a typical value for ionic diffusion coefficients in water, and δ is the boundary layer thickness which was set at 10 μm. The last is rather an upper limit, thus k_{diff} values could be even higher.

Another strong indication of rate control by slow surface reactions is given by the sensitivity of the rate constants towards acid concentration (Table I). Fig. 3 presents the pH dependence of log k, and shows that the apparent kinetic order on proton concentration

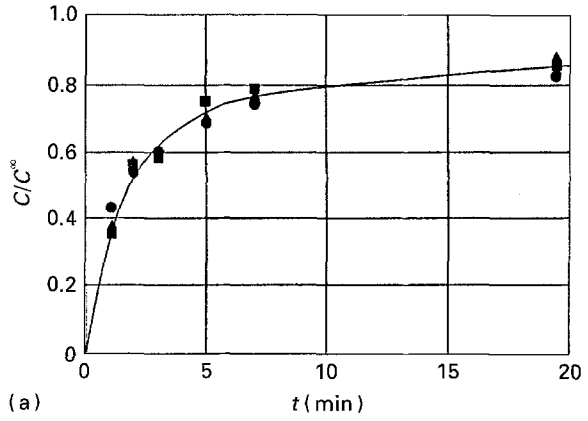

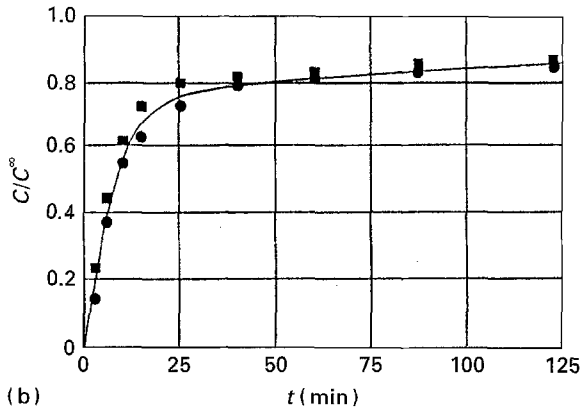

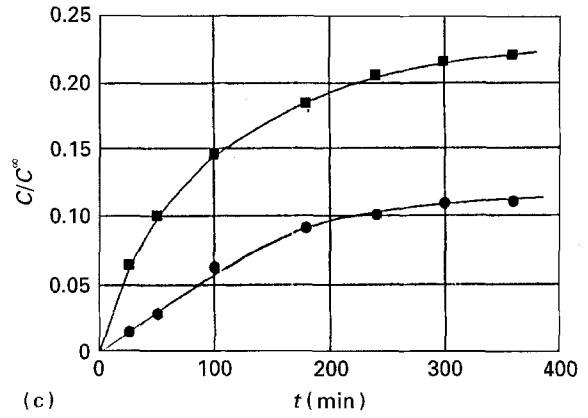

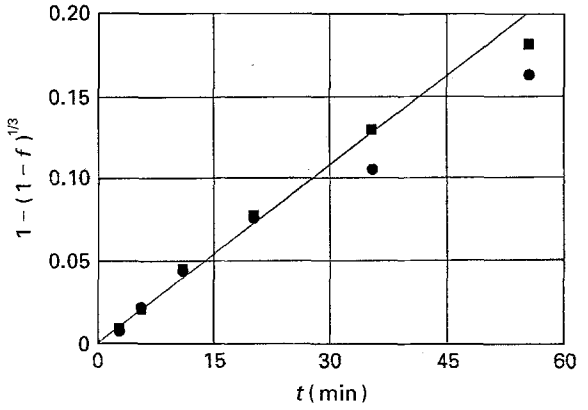

Figure 2 Time dependence of the function $[1-(1-f)^{1/3}]$ for the dissolution of $YBa_2Cu_3O_{6.8}$ in 1 mol dm^{-3} NaCl at pH 4.0; $T = 298$ K; (■) and (●) data points correspond to dissolved yttrium and copper, respectively; negative deviations from Equation 2 are not shown.

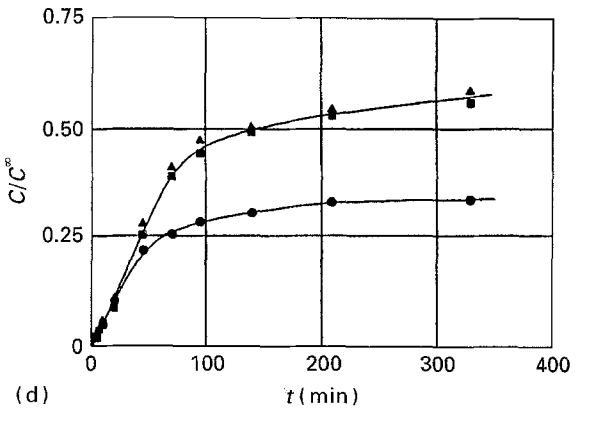

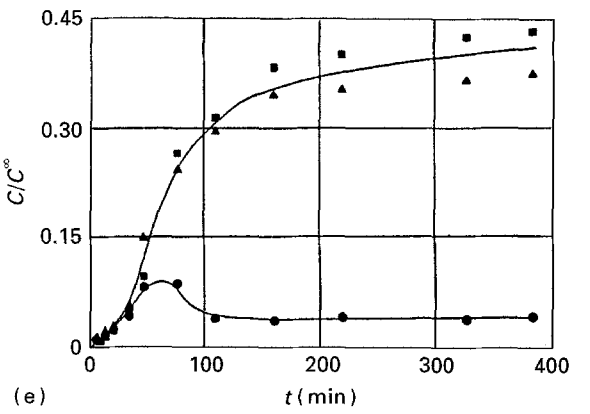

Figure 1 Concentrations of dissolved Ba (▲), Y (■) and Cu (●), expressed as dissolution fractions ($f = C/C^{\infty}$), as a function of reaction time: (a) pH 2.0, [NaCl] = 1 mol dm^{-3}; (b) pH 3.0, [NaCl] = 1 mol dm^{-3}; (c) pH 5.0, [NaCl] = 1 mol dm^{-3}; (d) pH 5.0, [NaCl] = 0; (e) pH 6.0, [NaCl] = 0; $T = 298$ K and in all cases pH was kept constant by the addition of HCl.

TABLE I Rate parameters characterizing the congruent dissolution of $YBa_2Cu_3O_{6.8}$ in 1 mol dm^{-3} NaCl solutions at 298 K

pH	k(s^{-1})	R_s(mol m^{-2} s^{-1})	p(cm s^{-1})
2.0	1.99×10^{-3}	3.72×10^{-6}	3.92×10^{-8}
3.0	4.44×10^{-4}	8.31×10^{-7}	8.75×10^{-9}
3.5	1.78×10^{-4}	3.33×10^{-7}	3.51×10^{-9}
4.0	5.63×10^{-5}	1.05×10^{-7}	1.11×10^{-9}

(see Equation 6) is not constant; it decreases with increasing acidity. This is a characteristic of surface controlled dissolution processes [24]

$$k = k_0[H^+]^n \quad (6)$$

One should note here that Rosamilia and coworkers [19] have found that the rate of dissolution of $YBa_2Cu_3O_7$ in acidic ($2.0 \geq$ pH ≥ 1.0) 1 mol dm^{-3} NaCl solutions is a linear function of proton concentration, e.g. $n = 1$. This finding, together with their earlier results of copper leaching from $YBa_2Cu_3O_7$ discs [18], led them to conclude that dissolution is controlled by the rate of diffusion of H^+ towards the

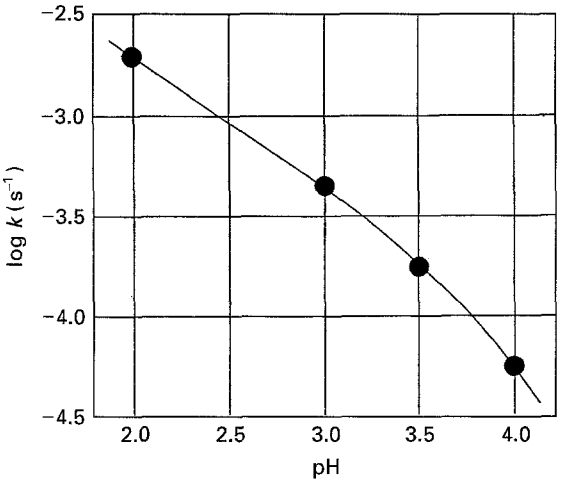

Figure 3 pH dependence of the contracting volume rate constant of the dissolution reaction of $YBa_2Cu_3O_{6.8}$ in 1 mol dm^{-3} NaCl at 298 K.

oxide surface; for $La_{1.8}Sr_{0.2}CuO_4$ [18], which dissolves at lower rates, mixed kinetic control was diagnosed. Kinetic control is obviously determined by the reactivity of the solid. The operation of surface chemical control in the present case is, indeed, in line with the reactivity trend $YBa_2Cu_3O_7 > YBa_2Cu_3O_{6.59}$ found by Zhou *et al.* [13].

Comparison of f versus t plots presented in Fig. 1a–c indicates that the dissolution behaviour of $YBa_2Cu_3O_{6.8}$ in 1 mol dm^{-3} NaCl solutions is appreciably different at the higher pH values. Fig. 1c shows that at pH 5.0 yttrium is leached faster than copper, and that leaching rates are arrested once a modest dissolution fraction has been achieved. A more detailed picture can be obtained from the data at low chloride concentrations that are depicted in Fig. 1d. In this case, higher dissolution rates are attained and dissolution is arrested at higher conversion values, ~ 0.30, 0.50 and 0.55 for Cu, Y and Ba, respectively. It is worth noting that the initial rates of dissolution of all three metal ions are similar; the order $R_{Ba} \approx R_Y > R_{Cu}$ (R_{Me} denoting the slope df/dt) becomes apparent once the value $f \approx 0.15$ has been reached. These results indicate that the combination of high pH and chloride concentration leads to lower rates and selective dissolution of Ba and Y as compared to Cu.

Fig. 1e is analogous to Fig. 1d, but corresponds to experiments carried out at pH 6.0. Here, the dissolution of copper is seen to be followed by its reprecipitation. Then, after 2 h, a rather passive condition is attained; the level of dissolved Cu remains low and the concentrations of Y and Ba reach rather constant values corresponding to $f \approx 0.40$. These observations clearly indicate that, in the higher pH range, a Cu-rich layer builds on top of the dissolving particles. The occurrence of the Cu-rich layer is demonstrated by EDX spectra of partially dissolved particles. Table II provides a summary of EDX results for runs performed at pH 4.0 and 5.0 in 1 mol dm^{-3} NaCl. As a reference, data for a sample briefly soaked in pure water are also given; they already show some copper

TABLE II EDX analyses of $YBa_2Cu_3O_{6.8}$ particles partially dissolved in 1 mol dm^{-3} NaCl solutions at 298 K

pH	t(h)	Cu:Y	Cu:Ba	Ba:Y
Pure water		3.8	1.7	2.3
4.0	0.04	4.1 (3.9)[a]	2.6 (2.6)	1.5 (1.5)
	4.00	100.0 (6.8)	300.0 (4.0)	0.5 (1.3)
5.0	0.26	4.2	1.9	2.2
	4.00	32.0 (6.1)	30.0 (4.7)	1.0 (1.5)

[a] Molar ratios given in parenthesis correspond to larger particles, showing a lesser degree of degradation.

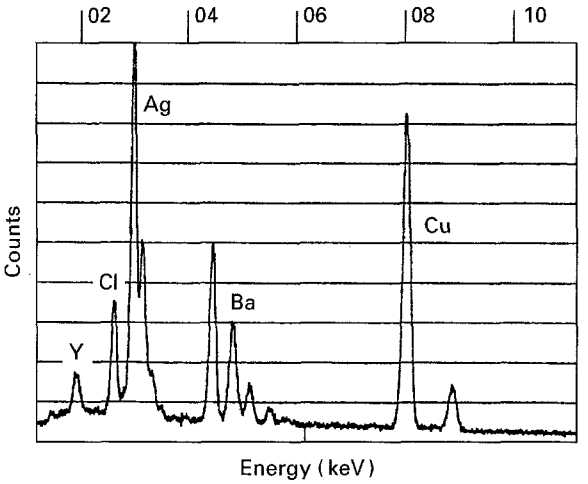

Figure 4 EDX spectrum of $YBa_2Cu_3O_{6.8}$ particles partially dissolved in 1 mol dm^{-3} NaCl at pH 5.0; t = 375 min; T = 298 K; note that the Ag peak results from the metallic coating of the inspected sample.

enrichment and barium depletion. EDX results also demonstrate that chloride is taken up by the solid surface (Fig. 4).

The above results indicate that copper basic chloride precipitates when Cu build up saturates the solution; the actual concentration to reach this point is a strong function of pH and chloride concentration. The interplay between copper leaching and reprecipitation rates determines whether the supersaturation seen in Fig. 1e is revealed.

The influence of the anion of the mineral acid is also largely related to the solubility of the corresponding basic salts. Fig. 5 compares the dissolution behaviour of $YBa_2Cu_3O_{6.8}$ in $HClO_4$, HNO_3, HCl and H_2SO_4 solutions of the same pH (5.0). These data were used to derive the rate constants listed in Table III. Since these systems do not comply with Equation 2, Table III presents the initial slopes casted in terms of $(df/dt)_{t\to 0}$ ($\equiv R_0$); R_0 is identical to $3k$. (As these rates were measured using the pH-state method, due allowance was made for the stoichiometric coefficients in Equation 1; the implicit assumption is that initial dissolution is congruent, cf. Fig. 1d.) Whereas R_0 values are not very sensitive to the different acids, the progress of the dissolution reaction is highly affected by the nature of the anions. In $HClO_4$ and HNO_3, 80 and 75% dissolution results after 2 h reaction time, and

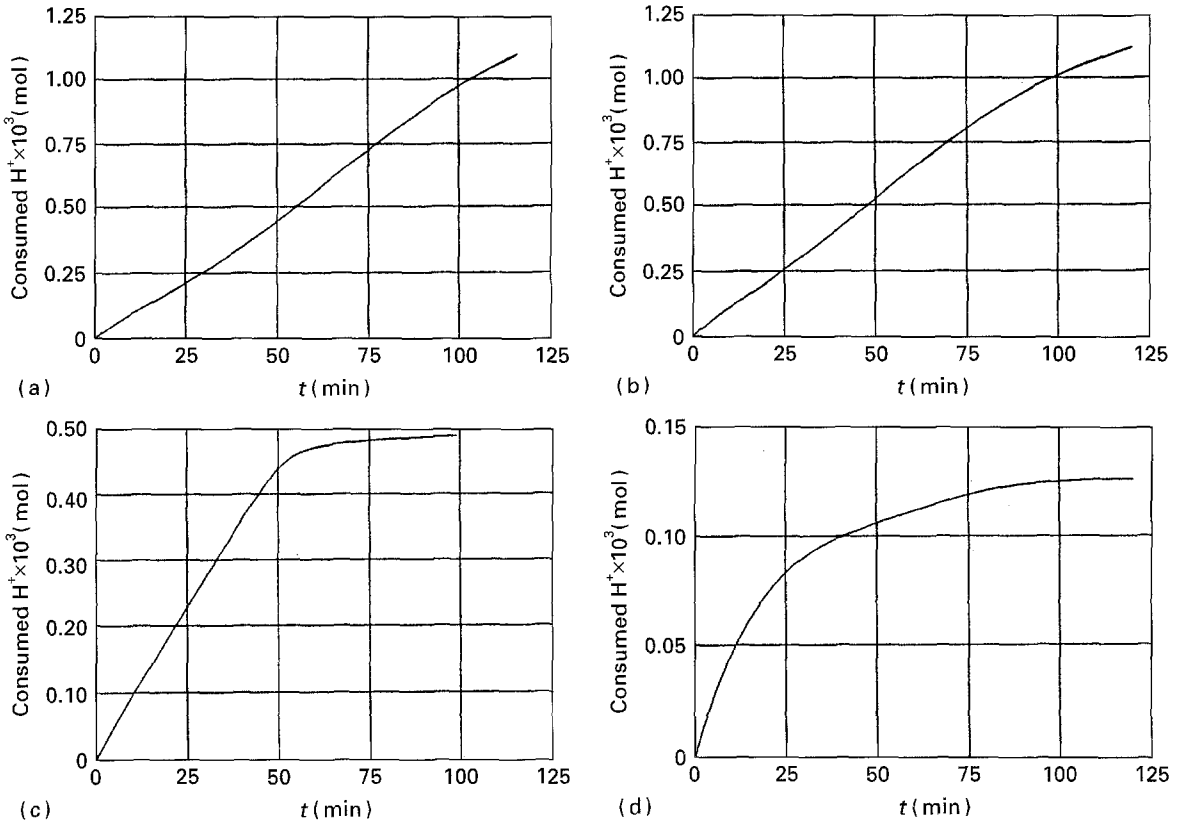

Figure 5 Proton consumption during the dissolution of $YBa_2Cu_3O_{6.8}$ in solutions of different mineral acids at pH 5.0; $T = 298$ K. (a) $HClO_4$, (b) HNO_3, (c) HCl, and (d) H_2SO_4.

TABLE III Characteristics of the dissolution behaviour of $YBa_2Cu_3O_{6.8}$ in different acid solutions at pH 5.0 and 298 K

Acid	$R_0 \times 10^4 (s^{-1})$	Conversion degree at passivation, f	Nature of passivating film[a]
$HClO_4$	0.9		
HNO_3	1.1		
HCl	1.0	34	$Cu_2(OH)_3Cl \cdot xH_2O$
H_2SO_4	0.4	9	$BaSO_4$

[a] As inferred from EDX.

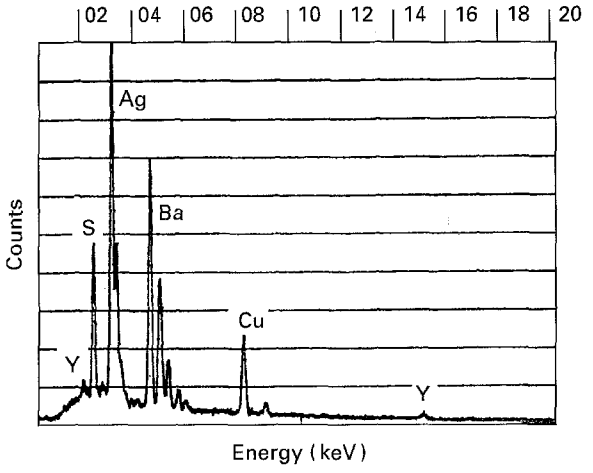

Figure 6 EDX spectrum of $YBa_2Cu_3O_{6.8}$ particles partially dissolved in a solution of constant pH (5.0) which was continuously adjusted by the addition of H_2SO_4; $t = 15$ h; $T = 298$ K; note that the Ag peak results from the metallic coating of the inspected sample.

extrapolation of the data predicts total dissolution at about 3 h; no signs of passivation are apparent. In HCl and H_2SO_4, on the other hand, dissolution is drastically arrested once dissolution factors of 0.34 and 0.09 are reached. (At the onset of reprecipitation, the associated change in the stoichiometry of Equation 1 influences only modestly the values of df/dt. Thus, the onset of reprecipitation may probably take place before f reaches these values, at which the rate is almost zero.) The observed trend is in line with the solubilities of copper basic salts. In the case of H_2SO_4, however, precipitation of $BaSO_4$, as evidenced by EDX (Fig. 6), leads to passivation.

4. Discussion

The attack of water on mixed oxides usually involves preferential lattice sites, that may either lead to incongruent dissolution, i.e. selective leaching of some components, or to congruent dissolution that may be followed by reprecipitation of more sparingly soluble solid phases. Even though metal ion concentration measurements are not sensitive enough to distinguish between these two mechanisms, the experimental results indicate that corrosion of $YBa_2Cu_3O_{6.8}$ in aqueous solutions proceeds through a congruent dissolution–reprecipitation mechanism (see, for instance, Fig. 1e); the same mechanism has been demonstrated to operate during the corrosion of barium titanate and related perovskitic phases [25]. The corrosion of a mixed oxide must certainly meet the thermodynamic constraints possed by the solubilities of the original phase and of the other possible solid phases that may

form. Thus, it is not surprising that the dissolution of $YBa_2Cu_3O_{6.8}$ will be arrested once an insoluble solid phase, e.g. copper basic chloride or barium sulphate; (cf. Table III) precipitates on top of the dissolving particles; further attack on the original solid requires diffusion across this passive layer. The nature of the passive layer is determined by pH and by the concentration and nature of the anions. In fact, the main role of anions seems to be their involvement in the formation of passive solids [20]. pH and concentration and nature of present anions are, therefore, the main variables that determine the extent of the dissolution reaction (see Figs 1 and 5). As a consequence of solubility constraints, the load of $YBa_2Cu_3O_{7-x}$ in the suspension becomes another important variable, for it also determines the f values required to saturate the solution, especially in media in which early precipitation of sparingly soluble corrosion products is possible. The following discussion will be essentially focused on the dissolution process itself.

At all studied pH values, dissolution is strongly dependent on solution pH (Fig. 3), and its rate is limited by a slow surface chemical reaction. Electrophilic attack of H_3O^+ on oxo bonds is a well documented process that usually takes place through protonation pre-equilibria followed by the slow release of cations [24]. In the surface complexation approach [24, 26–28], which has established the parallelism of surface and solution chemistry, surface protonation is described as a mass law process

$$\equiv Me{-}OH + H^+ \rightleftharpoons \equiv Me{-}OH_2^+ \qquad (7)$$

and protonated sites are identified as the surface entities promoting dissolution. Thus, the dissolution rate is given by

$$R_{Me} = k_{Me}^{SC}\{\equiv Me{-}OH_2^+\}^m \qquad (8)$$

where $\{\equiv Me{-}OH_2^+\}$ denotes surface concentration of protonated sites, k_{Me}^{SC} is the rate constant characterizing their reactivity, and m is the kinetic order on proton surface concentration; m is related to the probability of finding an ensemble of $m \equiv Me{-}OH_2^+$ vicinal groups [28]. This mechanism is further supplemented by the assumption that the transferred species are only unhydrolysed metal ions; this assumption predicts $m = z$, the charge number of the metal ions [29, 30]. Finally, the surface concentration of protonated sites is given by the Frunkin–Fowler–Guggenheim isotherm [28]

$$[H^+] = K_{al}^{int}\frac{\{\equiv Me{-}OH_2^+\}}{N_s - \{\equiv Me{-}OH_2^+\}} \times \exp\left[\frac{F^2\{\equiv Me{-}OH_2^+\}}{C_H RT}\right] \qquad (9)$$

where the reciprocal of K_{al}^{int} is the constant for the equilibrium depicted by Equation 7, N_s is the total number of available surface sites, F is the Faraday, C_H is the Helmholtz layer capacity and RT is the thermal energy. Combination of Equations 8 and 9 yields the apparent kinetic order on $[H^+]$, n (in Equation 6), as a fractional and variable number (see Fig. 3). (Surface controlled dissolution reactions of metal oxides can also be described in terms of the electrochemical model of Vermilyea [31] and Diggle [32]. They also predict a fractional, albeit constant, value for n, Equation 6.)

For mixed oxides, application of the surface complexation approach is not, however, straightforward. First, the proton affinity of the different surface metal ions is not the same. Second, k_{Me}^{SC} values are expected to differ since they reflect the lability of the different metal ions. In the present case, the basicities run in the order $Ba \gg Y \approx Cu$. Thus, variations of the overall surface charge should be dominated by the protonation of surface copper and yttrium ions, particularly, in the acidic media explored in this study. Nevertheless, owing to the high surface mobility of H^+, surface protonation may give rise to the phase transfer of any metal ion irrespective of surface speciation, if the corresponding k_{Me}^{SC} value is adequately high.

Among the three surface metal ions, barium ions are easily identified as the most reactive ones on the basis of site binding energies. Noteworthily, leaching of Ba^{2+} from Ba containing oxidic phases is a well known phenomenon; fast initial leaching of Ba^{2+} from $YBa_2Cu_3O_7$ has already been reported, and described as an ion exchange process [11]. This bond-breaking bond-making initial process gives rise to dramatic changes in the co-ordination environments of neighbouring surface metal ions, producing new highly activated sites; i.e. Cu and Y sites characterized by larger k_{Cu}^{SC} and k_Y^{SC} values. Thus, Y and Cu dissolution follow immediately, and a steady state, in which the individual R_{Me} values become equal, is soon attained. In agreement, Fig. 1 demonstrates that Ba, Y and Cu dissolve all at the same rate; the exception, Fig. 1c, corresponds to high pH and chloride concentration, where the passive layer forms at very low f values. The higher reactivity of barium sites thus renders a steady state surface composition that is enriched in copper and also in yttrium (see, for instance, the data in Table II for very short reaction times).

These effects can, in principle, be introduced explicitly in the surface complexation formalism (Equations 7–9), but its actual application requires of experimentally determined surface charge versus pH data, an inaccessible experimental information for highly reactive oxides, such as $YBa_2Cu_3O_{7-x}$. Nevertheless, the concepts underlying the surface complexation approach account well for the observed dissolution behaviour.

Although the above picture would suffice to describe the experimental results, it is clear that the presence of the formal oxidation state Cu(III) must play an important role in defining dissolution rates. The high oxidizing power of Cu(III) surface ions should certainly be reflected as an increased ability to phase transfer [as compared with Cu(II) surface sites]. In fact, CuO dissolves faster in oxidizing media [33, 34]. NiO also dissolves faster in the presence of oxidants because the availability of holes (either, mobile or trapped as Ni^{3+} or O^-) is increased [24]. Availability of charge carriers must also define the lability of surface copper ions in both CuO and $YBa_2Cu_3O_{7-x}$; it is already known that Ni(III) and Cu(III) behave similarly (see, e.g. [35]). Therefore, two

parallel Cu dissolution pathways can be envisaged. They are sketched in the kinetic scheme presented by Equation 10

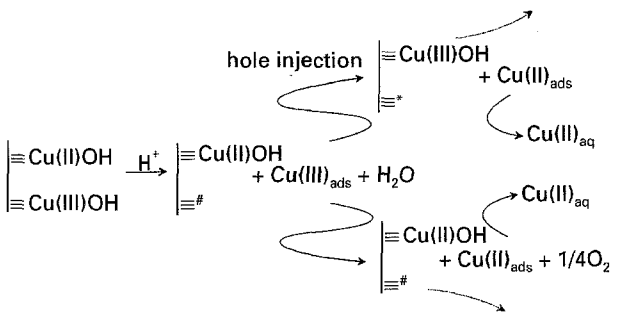

(10)

In this scheme, $\equiv^{\#}$ and $\equiv^{*}$ denote activated sites left behind by copper phase transfer and the subscript *ads* indicates adsorbed species; charges were omitted for simplicity. This scheme accounts for several experimental observations: the increasing reactivity of orthorhombic $YBa_2Cu_3O_{7-x}$ of decreasing x [13], the noted reduction of Cu(III) which takes place within the diffusion layer of dissolving $YBa_2Cu_3O_7$ discs [18], and the frequently reported oxygen evolution [6]. It also accounts for the evidence advanced by Salvador *et al.* [36] supporting that surface Cu(III) ions oxidize surface O^{2-} ions in a water promoted reaction, e.g.

$$2 \equiv Cu^{3+} + 2 \equiv O^{2-} + H_2O \rightarrow 2 \equiv Cu^{2+} + 2 \equiv OH^- + 0.5O_2 \quad (11)$$

Oxygen evolution will certainly render highly activated sites which will prompt phase transfer of Cu(II); hence, it will also increase the lability of the other surface metal ions.

Equations 10 and 11 involve localized holes, which have been described as Cu(III). The alternative view of O^- species leads to equivalent descriptions.

Acknowledgements

This work was partially supported by Universidad de Buenos Aires. The authors are indebted to E. Baran, who kindly provided the $YBa_2Cu_3O_{6.8}$ specimen. The assistance of R. T. Gettar, E. A. Gautier, R. Crubelatti, P. Smichowski (IC and AAS), P. Konig (XRD) and M. Villegas (EDX) is gratefully acknowledged. M. A. B. and A. E. R. are members of CONICET.

References

1. S. MYHRA, D. K. PHAM, R. St C. SMART and P. S. TURNER, in "Science of Ceramic Interfaces", edited by J. Nowotny (Elsevier, Amsterdam, 1991) p. 569.
2. A. BARKATT, H. HOJAJI, V. R. W. AMARAKOON and J. G. FAGAN, *Mater. Res. Soc. Bull.* September (1993) 45.
3. B. G. HYDE, J. G. THOMPSON, R. L. WITHERS, J. D. FITZGERALD, A. M. STEWART, D. J. M. BEVAN, J. S. ANDERSON, J. BITMEAD and M. S. PATERSON, *Nature* **327** (1987) 402.
4. J. G. THOMPSON, B. G. HYDE, R. L. WITHERS, J. S. ANDERSON, J. D. FITZGERALD, J. BITMEAD, M. S. PATERSON and A. M. STEWART, *Mater. Res. Bull.* **22** (1987) 1715.
5. J. WANG, R. STEVENS and J. BULTITUDE, *J. Mater. Sci.* **23** (1988) 3393.
6. N. P. BANSAL and A. L. SANDKUHL, *Appl. Phys. Lett.* **52** (1988) 323.
7. H. S. HOROWITZ, R. K. BORDIA, R. B. FLIPPEN, R. E. JOHNSON and U. CHOWDHRY, *Mater. Res. Bull.* **23** (1988) 821.
8. S. G. JIN, L. G. LIU, Z. Z. ZHU and Y. L. HUANG, *Solid State Commun.* **69** (1989) 179.
9. Z. DEXIN, X. MINGSHAN, Z. ZIQING, Y. SHUBIN, Z. HUANSUI and S. SHUXIA, *ibid.* **65** (1988) 339.
10. J. DOMINEC, L. SMRČKA, P. VAŠEK, S. GEURTEN, O. SMRČKOVÁ, D. SÝKOROVÁ and B. HÁJEK, *ibid.* **65** (1988) 373.
11. D. K. PHAM, Z. RUPENG, P. E. FIELDING, S. MYHRA and P. S. TURNER, *J. Mater. Res.* **6** (1991) 1148.
12. Z. RUPENG, M. J. GORINGE, S. MYHRA and P. S. TURNER, *Phil. Mag.* **A 66** (1992) 491.
13. J. P. ZHOU, D. R. RILEY and J. T. McDEVITT, *Chem. Mater.* **5** (1993) 361.
14. J. T. McDEVITT, M. LONGMIRE, R. GOLLMAR, J. C. JERNIGAN, E. F. DALTON, R. McCARLEY, R. W. MURRAY, W. A. LITTLE, G. T. YEE, M. J. HOLCOMB, J. E. HUTCHINSON and J. P. COLLMAN, *J. Electroanal. Chem.* **243** (1988) 465.
15. S. ROCHANI, D. B. HIBBERT, S. X. DOU, A. J. BOURDILLON, H. K. LIU, J. P. ZHOU and C. C. SORRELL, *ibid.* **248** (1988) 461.
16. J. M. ROSAMILIA and B. MILLER, *ibid.* **249** (1988) 205.
17. *Idem, J. Electroanal. Soc.* **135** (1988) 3030.
18. J. M. ROSAMILIA, B. MILLER, L. F. SCHNEEMEYER, J. V. WASZCZAK and H. M. O'BRYAN, Jr, *ibid.* **134** (1987) 1863.
19. V. M. MAGEE, J. M. ROSAMILIA, T. K. KOMETANI, L. F. SCHNEEMEYER, J. V. WASZCZAK and B. MILLER, *ibid.* **135** (1988) 3026.
20. B. J. HEPBURN, H. L. LAU, S. B. LYON, R. C. NEWMAN, G. E. THOMPSON and N. ALFORD, *Corrosion Sci.* **33** (1992) 515.
21. R. CRUBELATTI, P. SMICHOWSKI, D. BATTISTONI, G. POLLA and E. MANGHI, *Solid State Commun.* **75** (1990) 101.
22. E. A. GAUTIER, R. T. GETTAR and R. E. SERVANT, *Anal. Chim. Acta* **6** (1988) 281.
23. G. A. URRUTIA and M. A. BLESA, *React. Solids* **6** (1988) 281.
24. M. A. BLESA, P. J. MORANDO and A. E. REGAZZONI, "Chemical Dissolution of Metal Oxides" (CRC Press, Boca Raton, FL, 1994).
25. S. MYHRA, R. St C. SMART and P. S. TURNER, *Scanning Microsc.* **2** (1988) 715.
26. W. STUMM, H. HOLH and F. DALANG, *Croat. Chem. Acta* **48** (1976) 491.
27. P. W. SCHINDLER and W. STUMM, in "Aquatic Surface Chemistry", edited by W. Stumm (Wiley, New York, 1987) Ch. 4.
28. E. WIELAND, B. WEHRLI and W. STUMM, *Geochim. Cosmochim. Acta* **52** (1988) 1969.
29. G. FURRER and W. STUMM, *ibid.* **50** (1986) 1847.
30. B. ZINDER, G. FURRER and W. STUMM, *ibid.* **50** (1986) 1861.
31. D. A. VERMILYEA, *J. Electrochem. Soc.* **113** (1966) 1067.
32. J. W. DIGGLE, in "Oxides and Oxide Films", Vol. 2, edited by J. W. Diggle (Marcel Dekker, New York, 1973) Ch. 4.
33. N. VALVERDE, *Ber. Bunsenges. Phys. Chem.* **80** (1976) 333.
34. N. P. SHEVELEV, J. G. GORICHEV, N. G. KLYUCHNIKOV and R. I. NASAROVA, *Russian J. Inorg. Chem.* **19** (1974) 931.
35. J. E. HUHEEY, "Inorganic Chemistry: Principles of Structure and Reactivity", Ch. 12, 2nd Edn (Harper & Row, New York, 1978).
36. P. SALVADOR, E. FERNÁNDEZ SÁNCHEZ, J. A. GARCÍA DOMÍNGUEZ, J. AMADOR, C. CASCALES and I. RASINES, *Solid State Commun.* **70** (1989) 71.

Received 15 February
and accepted 17 July 1995